Eur. Phys. J. D (2015) 69: 147
DOI: 10.1140/epjd/e2015-50858-4

THE EUROPEAN PHYSICAL JOURNAL D

Regular Article

Influences of initial states of a bath on the dynamics of central spin

Wen-Jian Yu[1], Bao-Ming Xu[1], Lin Li[1], Jian Zou[1,a], Hai Li[2], and Bin Shao[1]

[1] School of Physics, Beijing Institute of Technology, Beijing 100081, P.R. China
[2] School of Information and Electronic Engineering, Shandong Institute of Business and Technology, Yantai 264000, P.R. China

Received 30 November 2014 / Received in final form 17 February 2015
Published online 4 June 2015 –

Abstract. We investigate the dynamics of an electronic spin coupled to a bath of nuclear spins. We consider three types of initial states with different correlations between the system and the bath, i.e., quantum correlation, classical correlation, and no-correlation. Although the reduced density matrices of the central spin and the bath are the same for these three initial states, the dynamical behaviors of the system are rather different. Interestingly, we show that the quantum correlations of the initial state between the system and the bath can lead to an increase in the coherence of the system while the classical correlations and no-correlation can not. In addition, we find that the initial bath state has significant influences on the dynamics of the system, and the effects of the distribution of coupling constants on the central spin crucially depend on the initial state of the spin bath.

1 Introduction

The central spin model is the generic theoretical description for an electronic spin coupled to a nuclear bath of noninteracting spins [1–10]. It has been widely used for experimental and theoretical studies in the areas of quantum information processing [11–17] and quantum decoherence [18–26]. As we know that due to unavoidable interactions of the central spin with the surrounding nuclear spins quantum coherence of the central spin will disappear finally. Decoherence is the main obstacle to quantum computing and quantum information processing. The environment destroys quantum interferences of the system, and the unwanted influences of the environment reduce the advantages of the quantum computing methods. In this regard, a long spin decoherence time is desirable. Generally, the decoherence of the system depends on the intrinsic properties of the environment. For an initially fully polarized spin bath, the inhomogeneous couplings lead to decoherence only initially for a short time [2] and the dynamical behaviors of the central spin are insensitive to the overall shape of the distribution of the hyperfine interaction as long as the mean values and the degree of the inhomogeneity are the same [25]. The dynamics and the entanglement entropy of the central spin exhibit rather different behaviors between the initially unpolarized unentangled bath and the eigenstate of the total spin bath [8]. The decay behaviors of the central spin is pronounced with a decreasing polarization of the bath spins [11,12]. The results of reference [27] indicate that the use of the control of the nuclear spins distribution may be more practical for suppressing decoherence of the system. Also, it has been shown that the entanglement in the environment may suppress the decoherence process [28,29]. In addition, it is noted that the influences of the inhomogeneities are suppressed with increasing polarization for the initially randomly correlated bath states [30,31].

However, most of the previous studies concentrate on the dynamics of central spin with the system and environment being initially statistically independent. This assumption generally is too restrictive for the real physical system. Experimentally, it is often unavoidable to have some correlations which may play significant roles in the time evolution of the system. Therefore, one should not neglect initial correlations between the system and environment [32–34]. The influence of initial correlations on open-system dynamics has been recently under intensive study [35–48]. Significantly, the effect of initial correlations on the dynamics of the system has been observed experimentally by means of trace distance [43]. It has also been demonstrated that initial correlations have nontrivial features in the quantum tomography process [44], and the initial correlations have remarkable influences on the entanglement in a two-qubit system interacting with a family of baths [48]. In this paper, we will study the effect of initial system-bath correlations and the role of the initial bath state on the dynamics of the system. Firstly, we discuss the time evolution of the central spin associated with the initial system-bath correlations. Three types of initial states are considered: the first contains quantum

[a] e-mail: zoujian@bit.edu.cn

correlations, the second has classical correlations, and the third has no correlation. Significantly, we find that the initial system-bath correlations have remarkable influences on the dynamics of central spin. The quantum correlations of initial states can lead to the increase in coherence of the central spin. However, the coherence is reduced in the cases of initial states with classical correlations or no correlation. Then, in the case of initial product states between the system and bath, we find that the decoherence of the system is suppressed greatly when the initial bath states are the W state and Dicke state. Nevertheless, the decay of system occurs easily when the initial bath states are the completely mixed states. In addition, the influences of the distribution of the hyperfine interaction on the dynamics of the system crucially depend on the initial state of the spin bath.

The paper is organized as follows: in Section 2 we introduce the Hamiltonian of the hyperfine interaction and derive the dynamics for three types of initial correlations. In Section 3 we study the dynamics of the system for two different initial bath states. Finally, we summarize our findings in Section 4.

2 Effects of different types of initial system-bath correlations

We consider a central spin-$\frac{1}{2}$ particle coupled to a spin bath composed of N noninteracting spin-$\frac{1}{2}$ particles, and the Hamiltonian can be written as:

$$\hat{H} = \sum_{k}^{N} A_k \mathbf{S}\cdot\mathbf{I}_k, \tag{1}$$

where the central spin is denoted by $\mathbf{S}$, and $\mathbf{I}_k$ is the nuclear spins of the kth nucleus with $\mathbf{S} = (\sigma_x, \sigma_y, \sigma_z)$, $\mathbf{I}_k = (\sigma_x^k, \sigma_y^k, \sigma_z^k)$. A_k is the coupling parameter for the hyperfine interaction of central spin with the surrounding nuclear spins of the kth nucleus. Generally, A_k is proportional to the square modulus of the respective electronic wave function at the site of the nuclear spins and is therefore clearly spatially dependent,

$$A_k = A_0 \upsilon |\Psi(\boldsymbol{r}_k)|^2, \tag{2}$$

where A_0 is an overall coupling parameter and υ is the volume of the unit cell containing one nuclear spin. $\Psi(\boldsymbol{r}_k)$ is the electron envelope wave function at the location $\boldsymbol{r}_k$. We do not consider the direct dipolar interaction between the nuclear spins because it is weaker by orders of magnitude than the scale of the hyperfine coupling.

2.1 Case of homogeneous coupling constants

In this subsection, we consider homogeneous couplings of the central spin, i.e., $A_k = \frac{A}{2}\ \forall\ k$. Since the nuclei are identical and indistinguishable, we can consider the collective operators $J_x = \sum_k I_x^k$, $J_y = \sum_k I_y^k$, $J_z = \frac{1}{2}\sum_k I_z^k$. The Hamiltonian can be rewritten in the form:

$$\hat{H} = \frac{A}{2}(\sigma_x J_x + \sigma_y J_y + 2\sigma_z J_z) = \frac{A}{2}\mathbf{S}\cdot\mathbf{J}. \tag{3}$$

As usual, we introduce the lowering and the raising operators $\sigma_\pm = \frac{1}{2}(\sigma_x \pm i\sigma_y)$, $J_\pm = \sum_k I_\pm^k$ and $I_\pm^k = \frac{1}{2}(I_x^k \pm i I_y^k)$. Therefore, in this case the Hamiltonian can be expressed as:

$$\hat{H} = A(\sigma_+ J_- + \sigma_- J_+ + \sigma_z J_z). \tag{4}$$

In the following, we define $|j,m\rangle$ as:

$$|j,m\rangle = \sqrt{\frac{(j+m)!}{N!(j-m)!}}\left(\sum_k I_-^k\right)^{j-m}|1,1,\ldots,1\rangle, \tag{5}$$

where $j = \frac{N}{2}$ [49], $m = -j, -j+1, \ldots, j-1, j$, and $|1,1,\ldots,1\rangle$ is the full polarized state with all bath spins up. $|j,m\rangle$ represents the fully symmetrical state in which $j+m$ particles are in the upper level $|1\rangle$, and $j-m$ in the lower level $|0\rangle$. The action of the operators J_z and $J_\pm$ on $|j,m\rangle$ is given by:

$$J_z|j,m\rangle = m|j,m\rangle, \tag{6}$$

$$J_\pm|j,m\rangle = \sqrt{j(j+1) - m(m\pm 1)}|j,m\pm 1\rangle. \tag{7}$$

In order to investigate the effects of different initial system-bath correlations on the dynamics of central spin, we consider three types of initial states,

$$\rho_{SE}^1 = (\alpha|\mu\rangle|j,m\rangle + \beta|\nu\rangle|j,m+1\rangle) \times (\alpha^*\langle\mu|\langle j,m| + \beta^*\langle\nu|\langle j,m+1|), \tag{8}$$

$$\rho_{SE}^2 = |\alpha|^2|\mu\rangle\langle\mu| \otimes |j,m\rangle\langle j,m| + |\beta|^2|\nu\rangle\langle\nu| \otimes |j,m+1\rangle\langle j,m+1|, \tag{9}$$

$$\rho_{SE}^3 = \rho_S \otimes \rho_E, \tag{10}$$

where $|\alpha|^2 + |\beta|^2 = 1, (\alpha, \beta \neq 0)$. For simplicity, we choose the parameters $\alpha = \cos\theta$, $\beta = \sin\theta$ $(\theta \in [0,\pi])$. $|\mu\rangle = \cos\gamma|0\rangle + \sin\gamma|1\rangle$ $(\gamma \in [0,\pi])$, with the central spin down $|0\rangle$ and up $|1\rangle$. $|\nu\rangle = \sin\gamma|0\rangle - \cos\gamma|1\rangle$. ρ_S and ρ_E in equation (10) are given by:

$$\rho_S = \begin{pmatrix} |\alpha|^2\sin^2\gamma + |\beta|^2\cos^2\gamma & (|\alpha|^2 - |\beta|^2)\sin\gamma\cos\gamma \\ (|\alpha|^2 - |\beta|^2)\sin\gamma\cos\gamma & |\alpha|^2\cos^2\gamma + |\beta|^2\sin^2\gamma \end{pmatrix}, \tag{11}$$

$$\rho_E = \begin{pmatrix} |\alpha|^2 & 0 \\ 0 & |\beta|^2 \end{pmatrix}. \tag{12}$$

The initial states ρ_{SE}^1, ρ_{SE}^2, and ρ_{SE}^3 have quantum correlations, classical correlations, and no correlation respectively. It is noted that the three initial states have the same reduced density matrices for both the system and the bath, i.e., equations (11) and (12).

For these choices of initial states, the density matrix $\rho_{SE}(t)$ can be obtained and therefore the reduced density matrix $\rho_S(t) = \mathrm{Tr_E}[\rho_{SE}(t)]$ of the central spin can be

calculated, where the bath degree of freedoms are traced out. For these three initial states, the results of $\langle S^z(t)\rangle_\lambda$ and $\rho_{12}^\lambda(t)$ ($\lambda = 1, 2, 3$, correspond to above three initial states) are respectively:

$$\langle S^z(t)\rangle_1 = \langle S^z(t)\rangle_2 + \frac{4}{(1+2j)^2}\sqrt{(j-m)(1+j+m)} \times (1+2m)\sin^2\gamma\sin 2\theta\sin^2 gt, \quad (13)$$

$$\langle S^z(t)\rangle_2 = \frac{1}{(1+2j)^2}\Big\{\big[-2(2-4j(1+j)+4m(1+m)) \times \cos 2\gamma\cos 2\theta + 4((2+4m)\cos^2\gamma - \cos 2\theta)\big] \times \sin^2 gt\Big\} - \cos 2\gamma\cos 2\theta, \quad (14)$$

$$\langle S^z(t)\rangle_3 = \langle S^z(t)\rangle_2 - \frac{4}{(1+2j)^2}(1+2m)\cos 2\gamma\sin^2 2\theta\sin^2 gt. \quad (15)$$

$$\rho_{12}^1(t) = \Re\left[\rho_{12}^2(t)\right] - \frac{1}{(1+2j)^2}\sqrt{(j-m)(1+j+m)} \times (1+2m)\sin 2\theta\sin 2\gamma\sin^2 gt + i\Big\{\Im\left[\rho_{12}^2(t)\right] - \frac{1}{2+4j}\sqrt{(j-m)(1+j+m)} \times \sin 2\theta\sin 2\gamma\sin 2gt\Big\}, \quad (16)$$

$$\rho_{12}^2(t) = \frac{\sin 2\gamma}{2(1+2j)^2}\Big\{(1+2j)^2\cos 2\theta\cos^2 gt - (1+2m)(-2+(1+2m)\cos 2\theta)\sin^2 gt\Big\} - \frac{i}{2+4j}\sin 2\gamma\sin 2gt[-1+(1+2m)\cos 2\theta], \quad (17)$$

$$\rho_{12}^3(t) = \Re\left[\rho_{12}^2(t)\right] - \frac{1}{(1+2j)^2}(1+2m)\sin^2 2\theta\sin 2\gamma\sin^2 gt + i\Big\{\Im\left[\rho_{12}^2(t)\right] - \frac{1}{2+4j}\sin^2 2\theta\sin 2\gamma\sin 2gt\Big\}, \quad (18)$$

where $\Re[\rho_{12}^2(t)]$ and $\Im[\rho_{12}^2(t)]$ are the real and imaginary part of $\rho_{12}^2(t)$ respectively, $g = A(1+2j)/2$. From these expressions, we find that the time evolution of $\langle S^z(t)\rangle$ and $|\rho_{12}(t)|$ for these three initial states are periodical and symmetric with respect to $\gamma = \frac{\pi}{2}$, so that we only consider $\gamma \in [0, \frac{\pi}{2}]$ and $\theta \in [0, \pi]$. From the above formulas, all physical quantities are strictly periodic because the simple structure of the Hamiltonian leads to an eigenvalue spectrum in which all transition frequencies (energy differences) are commensurate.

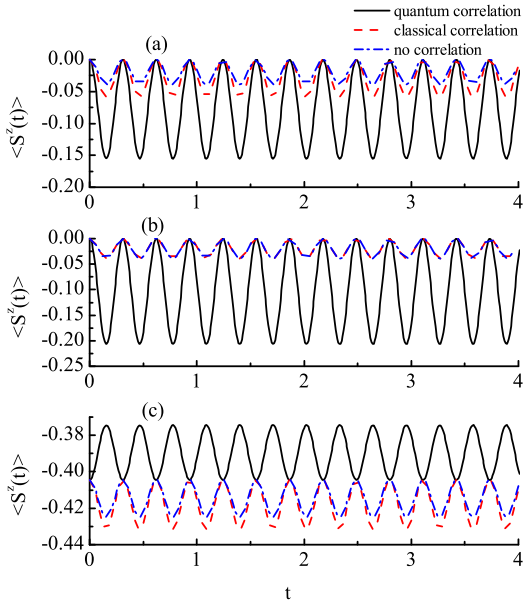

Fig. 1. Time evolution of $\langle S^z(t)\rangle$ as a function of t for three types of initial correlations. (a) $\theta = \frac{\pi}{4}$ and $\gamma = \frac{\pi}{6}$, (b) $\theta = \frac{\pi}{3}$ and $\gamma = \frac{\pi}{4}$, (c) $\theta = \frac{9\pi}{10}$ and $\gamma = \frac{\pi}{6}$. (i) ρ_{SE}^1 (black solid line); (ii) ρ_{SE}^2 (red dash line); (iii) ρ_{SE}^3 (blue dash dot line). The number of nuclear spins in the bath $N = 100$ and $m = -50$. The coupling constant $A = 0.2$.

It is noted that in the present paper we assume $j = \frac{N}{2}$. From equations (13)–(15) and (16)–(18), we find that for $m = 0$ the dynamical behaviors of $\langle S^z(t)\rangle$ and $|\rho_{12}(t)|$ for ρ_{SE}^1, ρ_{SE}^2 and ρ_{SE}^3 are similar in the case of larger N, in which,

$$\langle S^z(t)\rangle_1 \approx -\cos 2\gamma\cos 2\theta\cos^2 gt + \mathcal{O}\left(\frac{1}{N}\right),$$
$$\langle S^z(t)\rangle_2 \approx \langle S^z(t)\rangle_3 \approx -\cos 2\gamma\cos 2\theta\cos^2 gt,$$

and

$$\left|\rho_{12}^1(t)\right| \approx \left|\frac{1}{2}\sin 2\gamma\cos 2\theta\cos^2 gt + \mathcal{O}\left(\frac{1}{N}\right)\right|,$$
$$\left|\rho_{12}^2(t)\right| \approx \left|\rho_{12}^3(t)\right| \approx \left|\frac{1}{2}\sin 2\gamma\cos 2\theta\cos^2 gt\right|.$$

Hence, we conclude that the initial system-bath correlations will vanish with m approaching zero. On the other hand, we can understand this phenomenon from that the third term of equation (4) has considerable influences on the dynamics of system for initial states with system-bath correlations for $m \neq 0$, nevertheless, it does not contribute to the dynamics for $m = 0$ due to the eigenvalue being 0 in equation (6). Therefore, the influences of the initial correlations will disappear with a larger number of nuclear spins N for $m = 0$. In this paper, in order to investigate the difference between these three initial states we mainly consider the case of $m = -\frac{N}{2}$.

In Figure 1, we plot $\langle S^z(t)\rangle$ for initial states ρ_{SE}^1, ρ_{SE}^2 and ρ_{SE}^3, (a) $\theta = \frac{\pi}{4}$ and $\gamma = \frac{\pi}{6}$, (b) $\theta = \frac{\pi}{3}$ and $\gamma = \frac{\pi}{4}$,

(c) $\theta = \frac{9\pi}{10}$ and $\gamma = \frac{\pi}{6}$. We can see that $\langle S^z(t)\rangle$ displays periodic oscillatory behaviors. The initial value of $\langle S^z(t)\rangle$ is the maximum in the process of evolution for the initial states ρ^2_{SE} and ρ^3_{SE}. It is noted that the average value of $\langle S^z(t)\rangle_2$ is larger than $\langle S^z(t)\rangle_1$ in Figure 1a. However, the average value of $\langle S^z(t)\rangle_1$ is larger than $\langle S^z(t)\rangle_2$ in Figure 1c. The above phenomena can be understood as follows: from equation (13), we find that $\langle S^z(t)\rangle_1$ is larger than $\langle S^z(t)\rangle_2$ when $(1+2m)\sin 2\theta > 0$ and vice versa, i.e., for fixed m the difference between the initial quantum correlations and the classical correlations associates with the sign of $\alpha\beta$ ($\alpha = \cos\theta$, $\beta = \sin\theta$) for $\langle S^z(t)\rangle$. When $\alpha\beta < 0$ there is a relative phase π between the basis vectors $|\mu\rangle|j,m\rangle$ and $|\nu\rangle|j,m+1\rangle$, while there is no relative phase for $\alpha\beta > 0$. On the other hand, comparing Figures 1a and 1c, we can see that the variation of parameter θ has obvious influence on the amplitudes of $\langle S^z(t)\rangle$, especially for the initial state ρ^1_{SE}. The difference between amplitudes of ρ^1_{SE} and ρ^3_{SE} is larger than that between ρ^2_{SE} and ρ^3_{SE}. From Figure 1 it can be seen that the difference is the largest when $\theta = \frac{\pi}{4}$ for fixed γ.

In order to further explain the above phenomenon, we take $\gamma = \frac{\pi}{4}$. From equations (13)–(15) one has

$$\langle S^z(t)\rangle_1 = \frac{2\sin^2 gt}{(1+2j)^2}[-2\cos 2\theta + (2+\sqrt{(j-m)(1+j+m)}\sin 2\theta)(1+2m)], \tag{19}$$

$$\langle S^z(t)\rangle_2 = \langle S^z(t)\rangle_3 = \frac{2\sin^2 gt}{(1+2j)^2}[-2\cos 2\theta + 2(1+2m)]. \tag{20}$$

From equation (19), we find that for initial states with quantum correlation there is a parameter $(1+2m)\sin 2\theta \times \sqrt{(j-m)(1+j+m)}$ which is relatively large compared with the other terms in the numerator due to the fact that $j = \frac{N}{2}$, so that the variation of parameter θ has remarkable influence on the amplitude of $\langle S^z(t)\rangle_1$. From equation (20), in the cases of initial states having classical correlations and no correlation, the dynamical behaviors of the $\langle S^z(t)\rangle$ are the same for $\gamma = \frac{\pi}{4}$ (see Fig. 1b). On the other hand, we find that the difference of amplitudes between ρ^1_{SE} and ρ^2_{SE} (ρ^3_{SE}) is the largest when $\theta = \frac{\pi}{4}$, which can be seen by comparing equation (19) with equation (20). Physically, the degree of quantum correlation is dependent on θ, and the quantum correlation will be close to the maximum as θ approaches $\frac{\pi}{4}$. Hence we conclude that, compared with the initial classical correlations, the influences of the initial quantum correlations on $\langle S^z(t)\rangle$ are sensitive to the parameter θ.

As we know that the off-diagonal matrix element $\rho_{12}(t)$ represents the coherence of $\rho_S(t)$. To illustrate comprehensively the effect of initial correlations on the reduced density matrix, in Figure 2 we plot the off-diagonal element $|\rho_{12}(t)|$ of the reduced density matrix as a function of t for three initial states, $N = 100$, $\gamma = \frac{\pi}{6}$ and different θ. From equations (16)–(18), we find that $|\rho_{12}(t)|$ can be larger than its initial value in the process of time evolution for ρ^1_{SE}, while for the other two initial states ρ^2_{SE} and ρ^3_{SE} this phenomenon does not happen which can be seen from Figures 2b and 2c. Figure 2, $|\rho_{12}(t)|$ displays periodic oscillations as $\langle S^z(t)\rangle$ (see Fig. 1), the amplitude for ρ^1_{SE} is larger than ρ^2_{SE} and ρ^3_{SE}, and the oscillations for ρ^2_{SE} and ρ^3_{SE} are similar. In addition, we find that the difference of amplitudes between initial states ρ^1_{SE} and ρ^3_{SE} is maximal when $\theta = \frac{\pi}{4}$ (see Figs. 2a–2c).

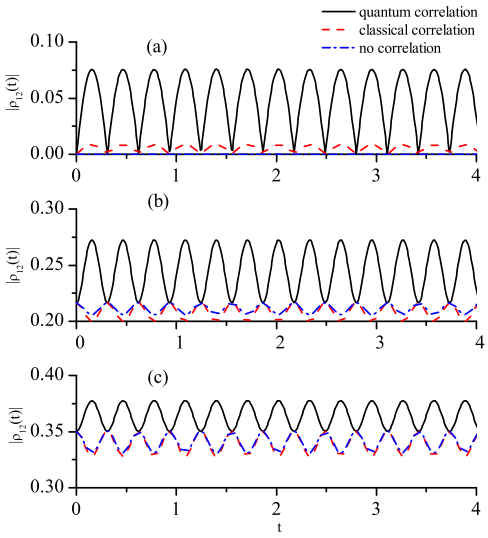

Fig. 2. Time evolution of $|\rho_{12}(t)|$ for three types of initial correlations. (a) $\theta = \frac{\pi}{4}$, (b) $\theta = \frac{\pi}{3}$, (c) $\theta = \frac{2\pi}{5}$. (i) ρ^1_{SE} (black solid line); (ii) ρ^2_{SE} (red dash line); (iii) ρ^3_{SE} (blue dash dot line), $\gamma = \frac{\pi}{6}$. $N = 100$, $m = -50$. The coupling constant $A = 0.2$.

In the following, in order to further study the dynamics of the off-diagonal element of the reduced density matrix $|\rho_{12}(t)|$, we consider $\theta = \frac{\pi}{4}$, then

$$\rho^1_{12}(t) = (1-\sqrt{(j-m)(1+j+m)})\left\{\frac{1}{(1+2j)^2}[(1+2m) \times \sin 2\gamma \sin^2 gt] + \frac{i}{2+4j}\sin 2gt \sin 2\gamma\right\}, \tag{21}$$

$$\rho^2_{12}(t) = \frac{1}{(1+2j)^2}\left[(1+2m)\sin 2\gamma \sin^2 gt\right] + \frac{i}{2+4j}\sin 2gt \sin 2\gamma, \tag{22}$$

$$\rho^3_{12}(t) = 0. \tag{23}$$

Obviously, the time evolutions of $|\rho_{12}(t)|$ are different for these three states. In the case of $\theta = \frac{\pi}{4}$, there is no off-diagonal element for initial states without any correlations in equation (23) which can be seen from Figure 2a. From equation (22), when initial states have classical correlations, the average value of $|\rho^2_{12}(t)|$ approaches 0 for a relatively large number of nuclear spins N ($j = \frac{N}{2}$) and has almost no oscillation. However, the amplitude of $|\rho_{12}(t)|$ is the largest for initial state ρ^1_{SE} compared with ρ^2_{SE} and ρ^3_{SE}. We can explain from equation (21) that the existence of the term $1-\sqrt{(j-m)(1+j+m)}$ can apparently lead to the variation in the amplitude of $|\rho^1_{12}(t)|$.

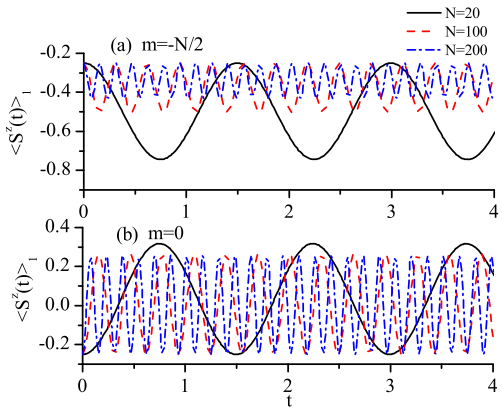

Fig. 3. Time evolution of $\langle S^z(t)\rangle$ for different numbers of nuclear spins. $N = 20, 100, 200$. (a) $m = -\frac{N}{2}$, (b) $m = 0$. The initial state is ρ^1_{SE}, $\theta = \gamma = \frac{\pi}{3}$. The coupling constant $A = 0.2$.

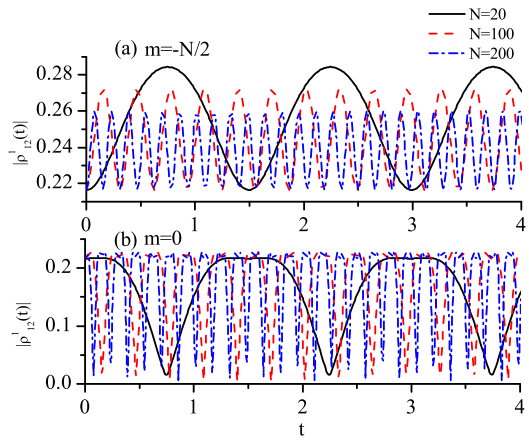

Fig. 4. Time evolution of $|\rho_{12}(t)|$ for different numbers of nuclear spins. $N = 20, 100, 200$. (a) $m = -\frac{N}{2}$, (b) $m = 0$. The initial state is ρ^1_{SE}, $\theta = \gamma = \frac{\pi}{3}$. The coupling constant $A = 0.2$.

Hence the initial quantum correlations have considerable influences on the off-diagonal elements of the reduced density matrix of central spin, and it can lead to an increase in coherence of the central spin. Physically, this can be understood as follows: for initial quantum correlations, the global coherence of the system and bath is redistributed into the central spin during the process of time evolution and it reaches the maximum for $\theta = \frac{\pi}{4}$ where the degree of quantum correlations are close to the maximum. The system can gain coherence with the initial quantum correlations unlike the cases for initial states having classical correlations and without any correlations.

Actually, a previous study [8] has calculated exactly the time-dependent reduced density matrix of the central spin with homogeneous couplings. It was shown that $\langle S^z(t)\rangle$ exhibits persistent monochromatic large-amplitude oscillations for the system and environment being initially statistically independent. For initial states with system-environment correlations our results are consistent with that of reference [8], and apart from that the off-diagonal matrix element $|\rho_{12}(t)|$ also exhibits persistent monochromatic large-amplitude oscillations.

Now we consider the influences of different numbers of nuclear spins N in the bath on the dynamics of the central spin. In Figures 3 and 4, we plot the time evolution of $\langle S^z(t)\rangle_1$ and the off-diagonal matrix element $|\rho^1_{12}(t)|$ with different N for ρ^1_{SE}, $m = -\frac{N}{2}$ and $m = 0$. Our analytical results show that with increasing number of nuclear spins N, the average values of $\langle S^z(t)\rangle_1$ and $|\rho^1_{12}(t)|$ approach the initial values which can be seen from Figures 3a and 4a. However, for $m = 0$ in Figures 3b and 4b we can see that the amplitude of oscillation is almost unaffected by the number of nuclear spins N. In equations (13) and (16), we have chosen $j = \frac{N}{2}$ and $g = A(1 + 2j)/2$, so that when $m = -\frac{N}{2}$,

$$\langle S^z(t)\rangle_1 \approx -\cos 2\gamma \cos 2\theta + \mathcal{O}\left(\frac{1}{\sqrt{N}}\right),$$
$$\left|\rho^1_{12}(t)\right| \approx \left|\frac{1}{2}\sin 2\gamma \cos 2\theta + \mathcal{O}\left(\frac{1}{N}\right)\right|,$$

and when $m = 0$, the expressions for $\langle S^z(t)\rangle_1$ and $|\rho^1_{12}(t)|$ have been given in previous discussion. From these expressions, we can see that with increasing N the average values of $\langle S^z(t)\rangle_1$ will approach the initial values ($t = 0$) for $m = -\frac{N}{2}$. Reference [8] has shown that the time evolution of $\langle S^z(t)\rangle$ exhibits this behavior with system and environment being initially statistically independent. This means that for initial states with quantum correlations our results are consistent with initial states where the system and environment are statistically independent. In addition, with increasing N the average value of off-diagonal matrix element $|\rho_{12}(t)|$ also approaches the initial values ($t = 0$) for $m = -\frac{N}{2}$. While when $m = 0$ the amplitudes of oscillations are almost identical for different N, irrespective of $\langle S^z(t)\rangle_1$ and $|\rho^1_{12}(t)|$(see Figs. 3b and 4b). For the initial states ρ^2_{SE} and ρ^3_{SE}, the influences of different numbers of nuclear spins on the dynamics of the system are similar to ρ^1_{SE}.

In conclusion, although the reduced density matrices of the central spin and the bath are the same for these three types of initial states, the dynamical behaviors of central spin are rather different. Compared with initial states having no correlation, the initial correlations have significant influences on the dynamics of central spin.

2.2 Case of inhomogeneous coupling constants

In the previous subsection, in order to obtain analytical results of the central spin model we consider the assumption of homogeneous hyperfine constants $A_k = \frac{A}{2}\ \forall\ k$ which is certainly a great simplification of the real physical situation. In this subsection, we will discuss the cases for different degrees of inhomogeneity by numerical simulation. We assume a Gaussian distribution with the site index k [3,25],

$$A_k = \frac{x_1 N e^{-\left(\frac{kB}{N}\right)^2}}{\sum_{k=1}^{N} e^{-\left(\frac{kB}{N}\right)^2}}, \tag{24}$$

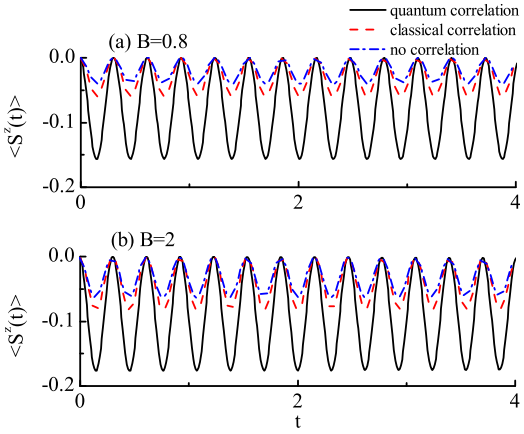

Fig. 5. Time evolution of $\langle S^z(t)\rangle$ for different values of parameter B. (a) $B = 0.8$, (b) $B = 2$. (i) ρ^1_{SE} (black solid line); (ii) ρ^2_{SE} (red dash line); (iii) ρ^3_{SE} (blue dash dot line). The number of nuclear spins in the bath $N = 100$, $m = -50$, $\theta = \frac{\pi}{4}$ and $\gamma = \frac{\pi}{6}$ which are the same as that in Figure 1a.

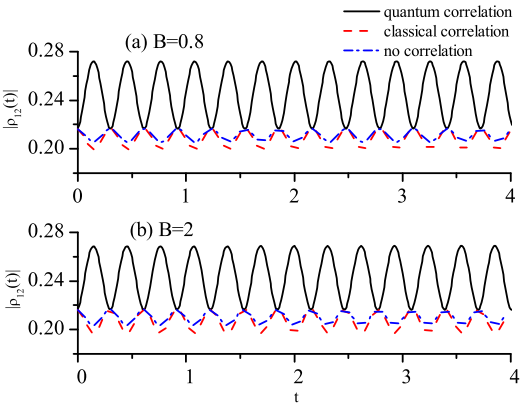

Fig. 6. Time evolution of $|\rho_{12}(t)|$ for different values of parameter B. (a) $B = 0.8$, (b) $B = 2$. (i) ρ^1_{SE} (black solid line); (ii) ρ^2_{SE} (red dash line); (iii) ρ^3_{SE} (blue dash dot line). The number of nuclear spins in the bath $N = 100$, $m = -50$, $\theta = \frac{\pi}{3}$ and $\gamma = \frac{\pi}{6}$ which are the same as that in Figure 2b.

which allows an easy control over the two relevant characteristics of the distribution of A_k, namely, the mean value $x_1 = \frac{\sum_k A_k}{N}$ and the degree of inhomogeneity B. We choose $x_1 = 0.1$, and $B = 2$ as a generic value for inhomogeneous couplings, and $B = 0.8$ as a parameter for nearly homogeneous couplings. It is noted that, the central spin model with inhomogeneous couplings was studied in reference [3], focusing on the spectral properties and static correlation functions in the ground state and excited states. Here we are interested in the influences of the initial system-environment correlations and different bath states on the dynamics of the central spin.

In Figures 5 and 6, we plot the time evolution of the $\langle S^z(t)\rangle$ and the off-diagonal element $|\rho_{12}(t)|$ for $m = -\frac{N}{2}$, $B = 0.8$ and $B = 2$. We can see that the time evolution of $\langle S^z(t)\rangle$ and $|\rho_{12}(t)|$ also displays the periodic oscillations. The influences of the three different initial correlations on the dynamics of system are similar among the cases of inhomogenous couplings constant ($B = 2$), nearly homogeneous couplings constant ($B = 0.8$), and the homogeneous couplings constant $A_k = \frac{A}{2}\ \forall\ k$. This can be seen by comparing Figures 1a and 5, Figures 2b and 6. In one word, for these three different initial states, the dynamics of central spin in inhomogenous and homogenous cases are similar for $m = -\frac{N}{2}$. It is noted that in reference [2] an analytical method based on the Bethe ansatz was introduced for the central spin model with inhomogeneous couplings. A simple example was considered, i.e., an initially fully polarized spin bath, which means that the whole system contains only one excitation. It was shown that for this initial state the inhomogeneous couplings lead to decoherence only for an initially short time. In order to study the initial system-environment correlations on the dynamics of the central spin in this paper we consider two excitations in the whole system. For more than one excitation, it is very difficult to obtain analytical results by using the method of reference [2].

3 Effect of different initial bath states on the dynamics of central spin

In order to clarify solely the role of the initial bath state in the dynamics of the system, in the following, we will discuss two different initial states of the spin bath, one is for completely mixed states and the other is for maximally entangled states. The state of the whole system of the former is given by the density matrix

$$\rho^4_{SE} = (C^N_{M_b})^{-1}|\mu\rangle\langle\mu| \otimes \mathcal{I}_{M_b}, \tag{25}$$

where we take the central spin to be in the state $|\mu\rangle$ which is the same as previously mentioned in equation (8), and the central spin and the bath are uncorrelated initially. $\mathcal{I}_{M_b}$ represents the completely mixed states of the bath, $C^N_{M_b} = \frac{N!}{M_b!(N-M_b)!}$ and M_b is the number of flipped spins in the bath. We will discuss the cases of $M_b = 1, 2$ in this section. Respectively, for the two initial maximally entangled states of the bath, the density matrices of the whole system are as follows:

$$\rho^5_{SE} = |\mu\rangle\langle\mu| \otimes |W\rangle\langle W|, \tag{26}$$

$$\rho^6_{SE} = |\mu\rangle\langle\mu| \otimes |D\rangle\langle D|. \tag{27}$$

We denote the ground state of nuclear spins as $|\widetilde{0}\rangle = |00\ldots0\rangle$ representing all spins in the down state and the W state $|W\rangle = (C^N_1)^{-\frac{1}{2}}(|100\ldots0\rangle + |010\ldots0\rangle + \ldots|000\ldots1\rangle) = (C^N_1)^{-\frac{1}{2}}\sum_{i=1}^{N}|W_i\rangle$ for the number of flipped spins $M_b = 1$ and the Dicke state $|D\rangle = (C^N_2)^{-\frac{1}{2}}\sum_{i,j=1}^{N}|D_{ij}\rangle$ for $M_b = 2$. Apparently, global coherences exist in the bath states corresponding to ρ^5_{SE} and ρ^6_{SE}, and not in the bath for ρ^4_{SE}.

In Figure 7, we plot the time evolution of $\langle S^z(t)\rangle$ for different values of parameter $B = 0$ (black solid line), $B = 0.8$ (red dash line) and $B = 2$ (blue dash dot line), $N = 20$, $\gamma = \frac{\pi}{3}$. We choose the initial states ρ^4_{SE} ($M_b = 1$)

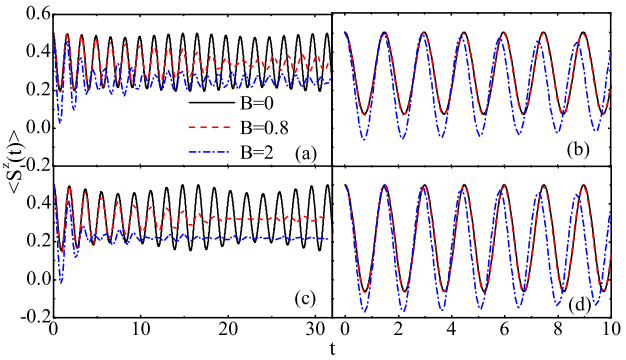

Fig. 7. Time evolution of $\langle S^z(t)\rangle$ for $N = 20$, $\gamma = \frac{\pi}{3}$, $x_1 = 0.1$, $M_b = 1$ (in (a) and (b)) and $M_b = 2$ (in (c) and (d)). The different initial states ρ^4_{SE} in (a) and (c), ρ^5_{SE} in (b) and ρ^6_{SE} in (d). Homogeneous coupling $B = 0$ (black solid line), nearly homogeneous coupling $B = 0.8$ (red dash line) and inhomogeneous coupling $B = 2$ (blue dash dot line).

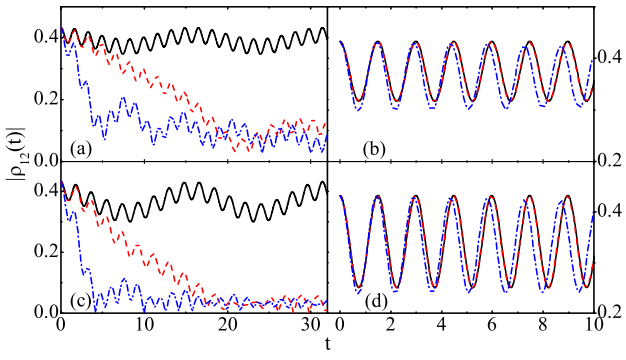

Fig. 8. Time evolution of $|\rho_{12}(t)|$ for $N = 20$, $\gamma = \frac{\pi}{3}$, $x_1 = 0.1$, $M_b = 1$ (in (a) and (b)) and $M_b = 2$ (in (c) and (d)). The different initial states ρ^4_{SE} in (a) and (c), ρ^5_{SE} in (b) and ρ^6_{SE} in (d). Homogeneous coupling $B = 0$ (black solid line), nearly homogeneous coupling $B = 0.8$ (red dash line), inhomogeneous coupling $B = 2$ (blue dash dot line).

in (a) and ρ^4_{SE} ($M_b = 2$) in (c), ρ^5_{SE} in (b) and ρ^6_{SE} in (d). We find that for the initial states ρ^4_{SE}, the evolution of $\langle S^z(t)\rangle$ will decay obviously by comparing the two left panels and two right panels, especially, in the cases of inhomogeneous couplings ($B = 2$, blue dash dot line) and nearly homogeneous couplings ($B = 0.8$, red dash line). The reason is that the entanglement in the bath protects the central spin from decohering for initial states ρ^5_{SE} and ρ^6_{SE}, so that the decay is not obvious in Figures 7b and 7d. In other words, the decoherence of central spin is suppressed by the presence of entanglement between the bath spins in initial states ρ^5_{SE} and ρ^6_{SE} which are maximally entangled. This phenomenon demonstrates that the entanglement in the bath can constrain entanglement between the central spin and bath, and hence limit the effect of decoherence. Actually, in references [28,29] it has established a relation between decoherence and entanglement inside the bath which is illustrated by using Ising model and our results are consistent with theirs.

Compared with the nearly homogeneous couplings, we find that the decay of $\langle S^z(t)\rangle$ becomes more pronounced in the case of inhomogeneous couplings for the initial state ρ^4_{SE} (see Figs. 7a and 7c), and with the increasing of B, the average values of $\langle S^z(t)\rangle$ become smaller. Figures 7b and 7d show that the variation of B has almost no effect on $\langle S^z(t)\rangle$ for the initial states ρ^5_{SE} and ρ^6_{SE}. Therefore, we can conclude that the effect of the inhomogeneous couplings on the central spin crucially depends on the state of the spin bath, i.e., the inhomogeneous couplings lead to the decoherence of the system and the decrease of the average values of $\langle S^z(t)\rangle$ for the initially completely mixed bath states, while for the initial W state and Dicke state the entanglement can constrain the effect of decoherence, irrespective of whether it is inhomogenous or homogeneous coupling.

In the following, we will investigate the influences of the initial bath states and the distribution of the coupling constants on the time evolution of off-diagonal element $\rho_{12}(t)$. Figure 8 shows the time evolution of $|\rho_{12}(t)|$ with the same parameters as given in Figure 7. Comparing the two left panels with two right panels of Figure 8, we find that the dynamical behaviors for the initial states ρ^5_{SE} and ρ^6_{SE} sharply contrast with ρ^4_{SE}. It is interesting that the decay occurs for initial state ρ^4_{SE}, and the average value of $|\rho_{12}(t)|$ is smaller obviously than that of initial states ρ^5_{SE} and ρ^6_{SE} for inhomogeneous couplings ($B = 2$) and nearly homogeneous couplings ($B = 0.8$). This phenomenon can be understood as the decay of the off-diagonal element of the central spin, which is also suppressed greatly by the initial entanglement between the bath spins for ρ^5_{SE} and ρ^6_{SE}, and the decay time is obviously extended.

In addition, comparing the black solid line, red dash line and blue dash dot line in Figures 8a or 8c one sees that $|\rho_{12}(t)|$ decreases more rapidly in the case of inhomogeneous couplings for the initially completely mixed states of the bath and the behaviors are different obviously for different B. Furthermore, we find that the distribution of the coupling constants almost does not influence $|\rho_{12}(t)|$ for the initial W state and Dicke state (see Figs. 8b or 8d). This is the same as the effect of the distribution of the coupling constants on $\langle S^z(t)\rangle$ (see Figs. 7b or 7d).

Apart from that, our numerical results show that the initial value of $|\rho_{12}(t)|$ is the maximum in the process of the evolution for the initial states ρ^4_{SE}, ρ^5_{SE} and ρ^6_{SE} which can be seen from Figure 8. Physically it can be explained as follows: the total coherence $\langle S^+\rangle + \sum_{k=1}^N \langle I_k^+\rangle$ is conserved due to the fact that $[S^+ + \sum_{k=1}^N I_k^+, \hat{H}] = 0$ in our model. The coherence of the system will be exchanged with that of the bath in the process of time evolution. However, for ρ^4_{SE}, ρ^5_{SE} and ρ^6_{SE}, $\sum_{k=1}^N \langle I_k^+\rangle = 0$, $\langle S^+\rangle \neq 0$ with $\gamma = \frac{\pi}{3}$, so that the coherence will be transferred into the bath from the central spin. In order to better illustrate this phenomenon, we take the central spin to be in $|1\rangle$, and the initial bath state to be in $|\widetilde{+}\rangle = (C_1^N)^{-\frac{1}{2}}(|+00\ldots0\rangle + |0+0\ldots0\rangle + \ldots |000\ldots+\rangle) = (C_1^N)^{-\frac{1}{2}} \sum_{i=1}^N |\widetilde{+}_i\rangle$ in Figure 9, where $|+\rangle = \frac{1}{\sqrt{2}}(|0\rangle + |1\rangle)$. We can see that the initial value of $|\rho_{12}(t)|$ is the minimum because the sum of initial local coherence of the

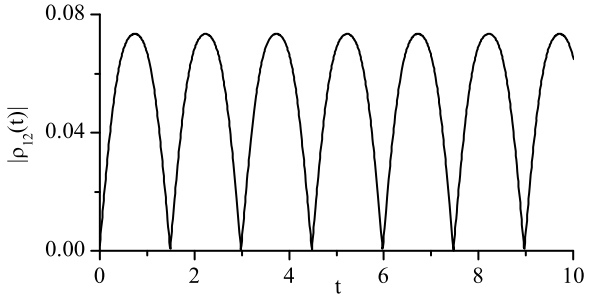

Fig. 9. Time evolution of $|\rho_{12}(t)|$ for initial state $|1\rangle \otimes |\widetilde{+}\rangle$, $\gamma = \frac{\pi}{2}$, $N = 20$, $x_1 = 0.1$. Homogeneous coupling $B = 0$.

bath states is nonzero with the initial bath state $|\widetilde{+}\rangle$, and the coherence of the central spin is zero with the initial state $|1\rangle$ in Figure 9. It is indicated that the coherence of the bath can be flowed into the system for suitable initial states.

In conclusion, the influences of the initial bath state and the hyperfine coupling constants are reflected obviously by $\langle S^z(t)\rangle$ and the coherence $|\rho_{12}(t)|$ of the central spin. We emphasize that the decoherence process of reduced density matrix $\rho_S(t)$ is suppressed in the case of initial bath states being in the W state and Dicke state, and the decay occurs obviously for the initially completely mixed bath states. On the other hand, it is noted that the effects of inhomogeneous couplings on the central spin crucially depend on the initial state of the spin bath. The inhomogeneous couplings lead to the decoherence of the system for the initially completely mixed bath states, while it has almost no effect on the dynamical behaviors of the system for the initial bath states being in the W state and Dicke state.

4 Conclusion

In this paper, we have considered three types of initial states with different correlations between the system and the bath: quantum correlation, classical correlation and no-correlation. We find that the influences of initial correlations on the dynamics of central spin are remarkable. Significantly, the quantum correlations of initial states between the system and the bath can lead to an increase in coherence of the central spin. However, the coherence is reduced in the cases of initial states having classical correlations and no correlation. For these three types of initial correlations, the dynamics of the system are similar with different distributions of hyperfine coupling constants in the case of $m = -\frac{N}{2}$. Apart from that, we have studied the influences of different initial bath states on the time evolution of the system. The decoherence of the central spin is supressed greatly for the initial bath state being in the W state or Dicke state and the decoherence time is obviously extended. However, the decay obviously occurs for the initially completely mixed bath states. Interestingly, we find that the effects of inhomogeneous couplings on the central spin crucially depend on the state of the spin bath. The inhomogeneous couplings lead to the decoherence of the system for the initially completely mixed bath states, while when the initial bath states are the W state and Dicke state the entanglement can constrain the effect of decoherence, irrespective of whether it is inhomogenous or homogeneous coupling.

This work is financially supported by the National Science Foundation of China (Grants Nos. 11274043, 11375025), the National Science Foundation of Shandong Province, China (Grant No. ZR2013AQ013), the Ph.D. research startup foundation of Shandong Institute of Business and Technology, China (Grant No. BS201418).

Wen-Jian Yu performed calculations, analysed the results and wrote the manuscript. Bao-Ming Xu analysed the results and helped in writing. Lin Li originated the idea and directed the project. Jian Zou originated the idea, directed the project, analysed the results and helped in writing. Hai Li offered help in plotting the graphics and Bin Shao contributed to editing the manuscript. All authors discussed the results and commented on the manuscript.

References

1. M. Gaudin, J. Phys. **37**, 1087 (1976)
2. M. Bortz, J. Stolze, Phys. Rev. B **76**, 014304 (2007)
3. M. Bortz, S. Eggert, J. Stolze, Phys. Rev. B **81**, 035315 (2010)
4. R. Hanson, L.P. Kouwenhoven, J.R. Petta, S. Tarucha, L.M.K. Vandersypen, Rev. Mod. Phys. **79**, 1217 (2007)
5. J. Fischer, W.A. Coish, D.V. Bulaev, D. Loss, Phys. Rev. B **78**, 155329 (2008)
6. J. Schliemann, Phys. Rev. B **81**, R081301 (2010)
7. E.A. Yuzbashyan, B.L. Altshuler, V.B. Kuznetsov, V.Z. Enolskii, J. Phys. A: Math. Gen. **38**, 7831 (2005)
8. M. Bortz, J. Stolze, J. Stat. Mech. **06**, P06018 (2007)
9. B. Erbe, H.J. Schmidt, J. Phys. A **43**, 085215 (2010)
10. A. Faribault, D. Schuricht, Phys. Rev. Lett. **110**, 040405 (2013)
11. J. Schliemann, A.V. Khaetskii, D. Loss, Phys. Rev. B **66**, 245303 (2002)
12. J. Schliemann, A.V. Khaetskii, D. Loss, J. Phys.: Condens. Matter **15**, R1809 (2003)
13. A.V. Khaetskii, D. Loss, L. Glazman, Phys. Rev. Lett **88**, 186802 (2002)
14. A.V. Khaetskii, D. Loss, L. Glazman, Phys. Rev. B **57**, 195329 (2003)
15. A. Hutton, S. Bose, Phys. Rev. A **69**, 042312 (2004)
16. Z.L. Xiang, S. Ashhab, J.Q. You, F. Nori, Rev. Mod. Phys. **85**, 623 (2013)
17. B. Urbaszek, X. Marie, T. Amand, O. Krebs, P. Voisin, P. Maletinsky, A. Högele, A. Imamoglu, Rev. Mod. Phys. **85**, 79 (2013)
18. N.V. Prokof'ev, P.C.E. Stamp, Rep. Prog. Phys. **63**, 669 (2000)
19. W.A. Coish, D. Loss, Phys. Rev. B **70**, 195340 (2004)
20. H.P. Breuer, D. Burgarth, F. Petruccione, Phys. Rev. B **70**, 045323 (2004)
21. Y. Hamdouni, M. Fannes, F. Petruccione, Phys. Rev. B **73**, 245323 (2006)
22. C.X. Deng, X.D. Hu, Phys. Rev. B **73**, R241303 (2006)

23. W.A. Coish, D. Loss, E.A. Yuzbashyan, B.L. Altshuler, J. Appl. Phys. **101**, 081715 (2007)
24. G. Chen, D.L. Bergman, L. Balents, Phys. Rev. B **76**, 045312 (2007)
25. M. Bortz, S. Eggert, C. Schneider, R. Stübner, J. Stolze, Phys. Rev. B **82**, R161308 (2010)
26. B. Erbe, J. Schliemann, Phys. Rev. B **81**, 235324 (2010)
27. W.X. Zhang, V.V. Dobrovitski, K.A. Al-Hassanieh, E. Dagotto, B.N. Harmon, Phys. Rev. B **74**, 205313 (2006)
28. C.M. Dawson, A.P. Hines, R.H. McKenzie, G.J. Milburn, Phys. Rev. A **71**, 052321 (2005)
29. D. Rossini, T. Calarco, V. Giovannetti, S. Montangero, R. Fazio, Phys. Rev. A **75**, 032333 (2007)
30. B. Erbe, J. Schliemann, Eur. Phys. Lett. **95**, 47009 (2011)
31. B. Erbe, J. Schliemann, Phys. Rev. B **85**, 155127 (2012)
32. P. Pechukas, Phys. Rev. Lett. **73**, 1060 (1994)
33. R. Alicki, Phys. Rev. Lett. **75**, 3020 (1995)
34. P. Pechukas, Phys. Rev. Lett. **75**, 3021 (1995)
35. T.F. Jordan, A. Shaji, E.C.G. Sudarshan, Phys. Rev. A **70**, 052110 (2004)
36. H.A. Carteret, D.R. Terno, K. Życzkowski, Phys. Rev. A **77**, 042113 (2008)
37. A. Shabani, D.A. Lidar, Phys. Rev. Lett. **102**, 100402 (2009)
38. A. Shabani, D.A. Lidar, Phys. Rev. A **80**, 012309 (2009)
39. A.R.U. Devi, A.K. Rajagopal, Phys. Rev. A **83**, 022109 (2011)
40. E.M. Laine, J. Piilo, H.P. Breuer, Eur. Phys. Lett. **92**, 60010 (2010)
41. M. Gessner, H.P. Breuer, Phys. Rev. Lett. **107**, 180402 (2011)
42. J. Dajka, J. Łuczka, Phys. Rev. A **82**, 012341 (2010)
43. A. Smirne, D. Brivio, S. Cialdi, B. Vacchini, M.G.A. Paris, Phys. Rev. A **84**, 032112 (2011)
44. K. Modi, E.C.G. Sudarshan, Phys. Rev. A **81**, 052119 (2010)
45. H.T. Tan, W.M. Zhang, Phys. Rev. A **83**, 032102 (2011)
46. Y.J. Zhang, X.B. Zou, Y.J. Xia, G.C. Guo, Phys. Rev. A **82**, 022108 (2010)
47. A.G. Dijkstra, Y. Tanimura, Phys. Rev. Lett. **104**, 250401 (2010)
48. L. Li, J. Zou, Z He, J.G. Li, B. Shao, L.A. Wu, Phys. Lett. A **376**, 913 (2012)
49. M. Gross, S. Haroche, Phys. Rep. **93**, 301 (1982)